Supplementary information of

LUCATOOv1 – A new land use change allocation tool and its application to the planetary boundary for land system change with the LPJmL

Arne Tobian et al.

Correspondence to: Arne Tobian (tobian@pik-potsdam.de)

S1 List of crop functional types

Table S1. The 16 crop functional types (CFTs) simulated in LPJmL5.1 (incl. 2 Bioenergy functional types).

Abbreviation	*Definition*	*Additional description*
TeCer	Temperate cereals	wheat, rye, barley
Rice	Rice	paddy rice; rice
Maize	Maize	maize for food; maize millet,
TrCer	Tropical cereals	sorghum
Pul	Pulses	pulses; field peas
TeRo	Temperate roots	sugar beet
TrRo	Tropical roots	cassava
SunFl	Sunflower	sunflower
Soy	Soybean	soybean
GrNu	Groundnut	groundnuts
Rape	Rapeseed	rapeseed
SuCa	Sugarcane	sugarcane
-	Others	potatoes, oil palm, citrus, date palm, grapes, cotton, cocoa, coffee, pastures, managed grasslands
-	Managed grasslands	
-	Bio-energy grass	
-	Bio-energy grasslands	

S2 Earth system processes affected by land use and land cover change

Freshwater change

Global terrestrial evapotranspiration is estimated to be reduced by 5.6% (~3,100 km^3 yr^{-1}), runoff increased by 7.6% (~3,900 km^3 yr^{-1}) and total soil moisture by 6% (14 kg m^{-3}), as a result of historic LULCC (Sterling et al., 2013). The altered terrestrial water flux to the atmosphere affects moisture recycling affecting precipitation patterns globally (van der Ent et al., 2010) which, in turn, leads to changes in plant available soil moisture, affecting plant growth and productivity (Wang-Erlandsson et al., 2022) and the terrestrial carbon sink (Humphrey et al., 2018).

Climate change

It is further estimated that LULCC contributes to climate change by being responsible for approximately 23% of greenhouse gas emissions (2007-2016), not only in the form of CO_2 but also through the emission of nitrous oxide and methane (accounted for as CO_2 equivalents) (IPCC, 2022). While CO_2 emissions originate mainly from deforestation (Friedlingstein et al., 2022), agricultural emissions of nitrous oxide stem predominantly from manure and fertilizer application, while methane is released by livestock's enteric fermentation and rice cultivation (IPCC, 2022). The global radiative balance is influenced by LULCC-induced changes in physical surface properties, such as changes in albedo, surface roughness and leaf surface area, altering the surface energy balance and surface temperature (Pongratz et al., 2021).

Atmospheric aerosol loading

LULCC alters the emissions of biogenic volatile organic compounds that contribute to the uncertainty of future climate change projections (Zhu et al., 2019).

Changes in biosphere integrity

By driving landscape fragmentation and subsequent habitat loss, LULCC is a primary driver of eroding the integrity of the terrestrial biosphere and pushes numerous species into extinction (Jantz et al., 2015).

Biogeochemical flows

Excessive fertilization and the application of manure significantly burden the nitrogen and phosphorus biogeochemical cycles within the Earth system and represent the primary contributor to non-CO_2 greenhouse gas emissions (IPCC, 2022). Soil erosion rates under agricultural land are >100 times higher (conventional tillage) than natural ecosystems (Montgomery, 2007). It is detrimentally affecting water quality (Issaka and Ashraf, 2017), aquatic and soil ecosystem health and nutrient availability (Guerra et al., 2020). The emerging dust from aeolian erosion is increasing the atmospheric aerosol loading with consequences for human health and Earth's radiative balance (Katra, 2020).

S3 IPCC reference region level

LUCATOO can be adjusted to operate on various spatial scales. Here we were testing to run in on the IPCC reference region level, following Iturbide et al. (2020).

I. Preprocessing

dropping of ocean regions (STP*, WIO*) → no land cells

dropping of Antarctica (ANT*) → not included in LPJmL

dropping of Arctic (ARC*) → no forest

dropping of small island regions (CAR*, NTP*, ETP*) → too few cells

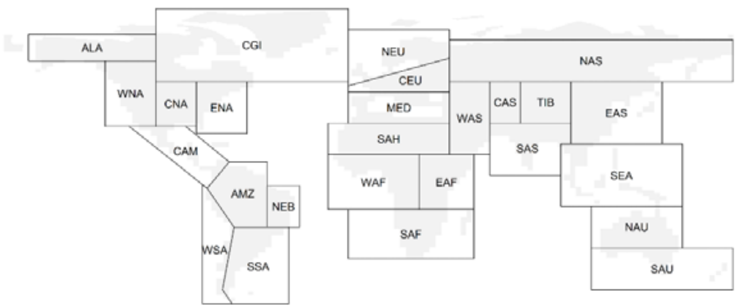

ALA:	Alaska/N.W. Canada	**EAS:**	East Asia	**SAH:**	Sahara
AMZ:	Amazon	**ENA:**	East North America	**SAS:**	South Asia
CAM:	Central America/Mexico	**MED:**	South Europe/Mediterranean	**SAU:**	South Australia/New Zealand
CAS:	Central Asia	**NAS:**	North Asia	**SEA:**	Southeast Asia
CEU:	Central Europe	**NAU:**	North Australia	**SSA:**	Southeastern South America
CGI:	Canada/Greenland/Iceland	**NEB:**	North-East Brazil	**TIB:**	Tibetan Plateau
CNA:	Central North America	**NEU:**	North Europe	**WAF:**	West Africa
EAF:	East Africa	**SAF:**	Southern Africa	**WAS:**	West Asia
				WNA:	West North America
				WSA:	West Coast South America

Figure S1: IPCC Reference regions matching the LPJmL grid.

II. Calculation of the current (2015) distribution and PB-LSC status for each biome in each IPCC reference region

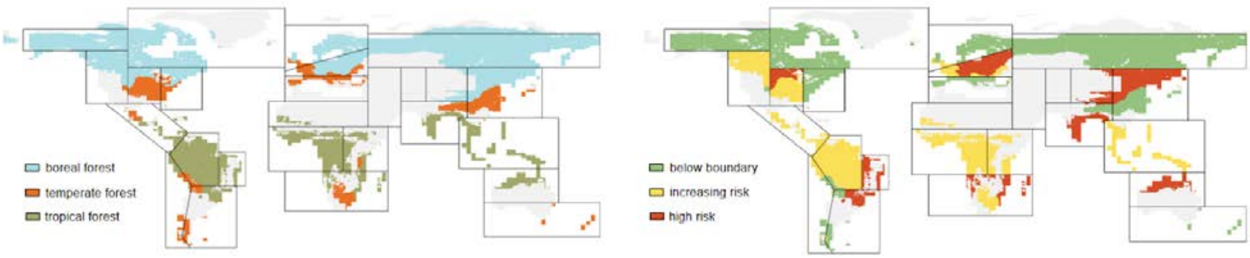

Figure S2: Biome distribution and PB-LSC status for IPCC reference regions.

III. Applying LUCATOO

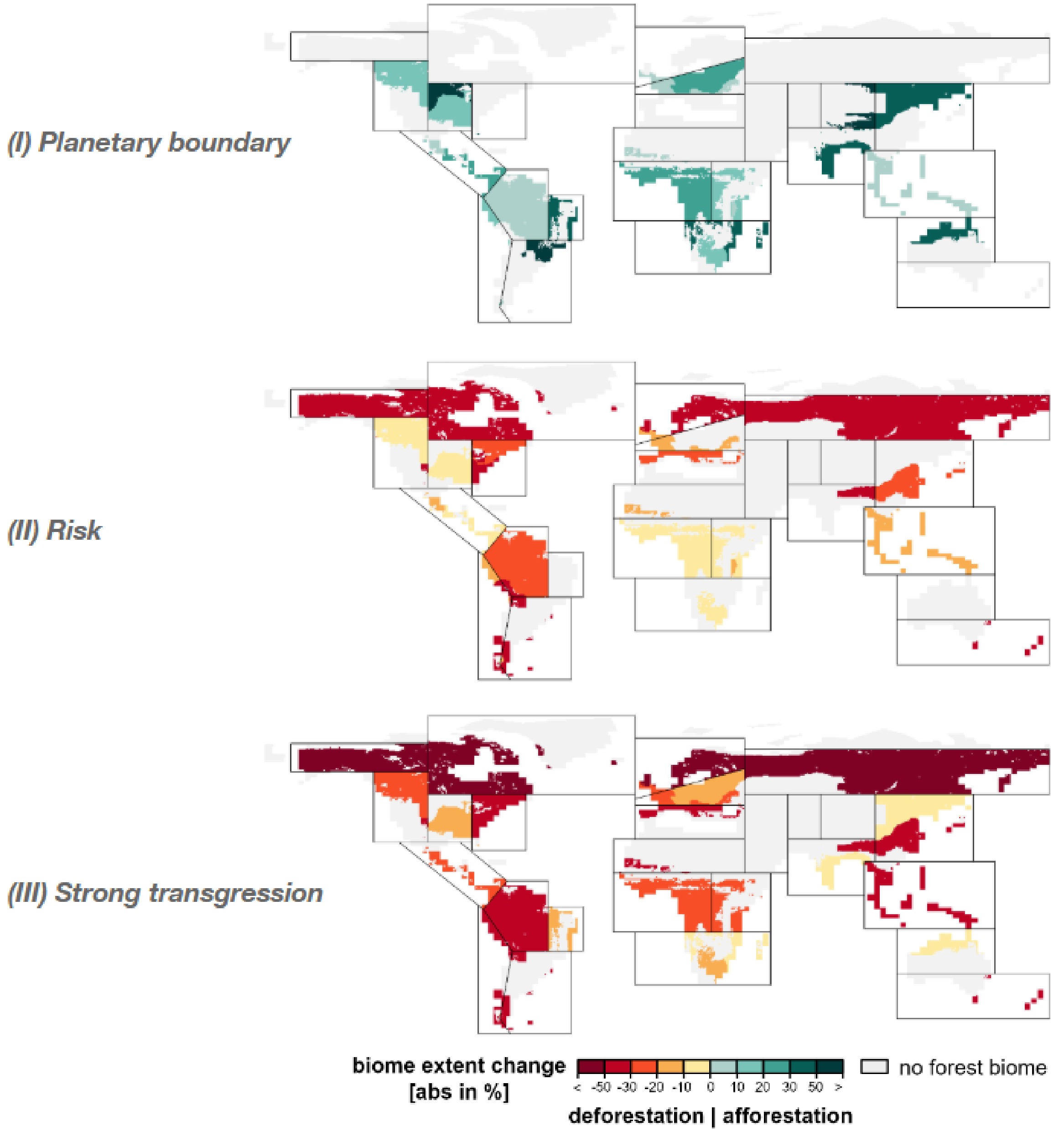

Figure S3: Running LUCATOO, adjusting LULCC to match PB-LSC transgression scenarios within IPCC reference regions.

60

S4 Premises and assumptions

For the calculation of the boundary status defined as the remainder of PNV forest extent, we used a simulated PNV extent as in earlier studies (Gerten et al., 2020; Heck et al., 2018; Tobian et al., 2024) both the PNV and historic LULCC simulations were conducted within the same modeling environment LPJmL to ensure consistency and comparability. Other studies, e.g. (Richardson et al., 2023; Steffen et al., 2015) have taken a different approach: they estimate the forest cover based on remote sensing imagery. This affects the extent of the forest biomes and their current status according to PB-LSC definition.

Second, our approach depends on the quality of the environmental factors dictating the distribution of forest biomes (climate data input forcing our LPJmL model) and the choice of the DGVM itself. Here, we use climate outputs from a single ESM, GFDL-ESM4. This model choice is justified as the ESM is included in the ISIMIP project (Frieler et al., 2017) and shows close to average equilibrium climate sensitivity and transient climate response when compared to the other models of the CMIP6 ensemble (Meehl et al., 2020). Future studies should, however, conduct an ensemble approach using multiple ESM outputs from CMIP6 (Eyring et al., 2016) to overcome ESM forcing uncertainty. The ESM-induced uncertainty over the historical period is, however, smaller than for future climate change scenarios (IPCC, 2023). We have chosen the LPJmL DGVM as it is state-of-the-art and well established featuring key processes needed for estimating the PB-LSC in a process-based manner. It is being constantly improved and extensively evaluated, e.g. the simulated vegetation cover against satellite imagery (Schaphoff et al., 2018). Moreover, the model version 5 employed here features nitrogen (von Bloh et al., 2018) potentially enabling studies targeted at the interactions of LULCC and biogeochemical cycles. The simulated biome distribution and forest extent - both initial requirements for our allocation tool - however are highly dependent on the employed DGVM and its representation of the underlying bioclimatic processes. Adjusting the tool to the output of multiple DGVMs of the ISIMIP-ensemble could significantly reduce the uncertainty arising from the DGVM choice (Frieler et al., 2017). While there are no comparative biome distributions studies from the ISIMIP ensemble, a study conducted by Ito et. al (2017) on GDP variability between DGVMs indicates that the simulated biome distributions are likely to vary significantly. Changes in biome distribution and extent are affecting both the PNV extent and PB-LSC status level. The PFT distribution simulated by the DGVM ultimately determines the need for afforestation / deforestation by our tool.

Next, the selected land use dataset and the uncertainties behind it directly affect the status of PB-LSC. This source of uncertainty propagates through the tool as the land use datafile constitutes its starting point.

Lastly, the postprocessing of the PFT distribution of our model via the applied biome classification algorithm is built on a set of assumptions. Here we employ a simplified biome classification algorithm based on Ostberg et al. (2013), as done in Tobian et al. (2024).

References

von Bloh, W., Schaphoff, S., Müller, C., Rolinski, S., Waha, K., and Zaehle, S.: Implementing the nitrogen cycle into the dynamic global vegetation, hydrology, and crop growth model LPJmL (version 5.0), Geosci. Model Dev., 11, 2789–2812, https://doi.org/10.5194/gmd-11-2789-2018, 2018.

van der Ent, R. J., Savenije, H. H. G., Schaefli, B., and Steele-Dunne, S. C.: Origin and fate of atmospheric moisture over continents, Water Resour. Res., 46, https://doi.org/10.1029/2010wr009127, 2010.

Eyring, V., Bony, S., Meehl, G. A., Senior, C. A., Stevens, B., Stouffer, R. J., and Taylor, K. E.: Overview of the Coupled Model Intercomparison Project Phase 6 (CMIP6) experimental design and organization, Geosci. Model Dev., 9, 1937–1958, https://doi.org/10.5194/gmd-9-1937-2016, 2016.

Friedlingstein, P., Jones, M. W., O'Sullivan, M., Andrew, R. M., Bakker, D. C. E., Hauck, J., Le Quéré, C., Peters, G. P., Peters, W., Pongratz, J., Sitch, S., Canadell, J. G., Ciais, P., Jackson, R. B., Alin, S. R., Anthoni, P., Bates, N. R., Becker, M., Bellouin, N., Bopp, L., Chau, T. T. T., Chevallier, F., Chini, L. P., Cronin, M., Currie, K. I., Decharme, B., Djeutchouang, L. M., Dou, X., Evans, W., Feely, R. A., Feng, L., Gasser, T., Gilfillan, D., Gkritzalis, T., Grassi, G., Gregor, L., Gruber, N., Gürses, Ö., Harris, I., Houghton, R. A., Hurtt, G. C., Iida, Y., Ilyina, T., Luijkx, I. T., Jain, A., Jones, S. D., Kato, E., Kennedy, D., Klein Goldewijk, K., Knauer, J., Korsbakken, J. I., Körtzinger, A., Landschützer, P., Lauvset, S. K., Lefèvre, N., Lienert, S., Liu, J., Marland, G., McGuire, P. C., Melton, J. R., Munro, D. R., Nabel, J. E. M. S., Nakaoka, S.-I., Niwa, Y., Ono, T., Pierrot, D., Poulter, B., Rehder, G., Resplandy, L., Robertson, E., Rödenbeck, C., Rosan, T. M., Schwinger, J., Schwingshackl, C., Séférian, R., Sutton, A. J., Sweeney, C., Tanhua, T., Tans, P. P., Tian, H., Tilbrook, B., Tubiello, F., van der Werf, G. R., Vuichard, N., Wada, C., Wanninkhof, R., Watson, A. J., Willis, D., Wiltshire, A. J., Yuan, W., Yue, C., Yue, X., Zaehle, S., and Zeng, J.: Global carbon budget 2021, Earth Syst. Sci. Data, 14, 1917–2005, https://doi.org/10.5194/essd-14-1917-2022, 2022.

Frieler, K., Lange, S., Piontek, F., Reyer, C. P. O., Schewe, J., Warszawski, L., Zhao, F., Chini, L., Denvil, S., Emanuel, K., Geiger, T., Halladay, K., Hurtt, G., Mengel, M., Murakami, D., Ostberg, S., Popp, A., Riva, R., Stevanovic, M., Suzuki, T., Volkholz, J., Burke, E., Ciais, P., Ebi, K., Eddy, T. D., Elliott, J., Galbraith, E., Gosling, S. N., Hattermann, F., Hickler, T., Hinkel, J., Hof, C., Huber, V., Jägermeyr, J., Krysanova, V., Marcé, R., Müller Schmied, H., Mouratiadou, I., Pierson, D., Tittensor, D. P., Vautard, R., van Vliet, M., Biber, M. F., Betts, R. A., Bodirsky, B. L., Deryng, D., Frolking, S., Jones, C. D., Lotze, H. K., Lotze-Campen, H., Sahajpal, R., Thonicke, K., Tian, H., and Yamagata, Y.: Assessing the impacts of 1.5 °C global warming – simulation protocol of the Inter-Sectoral Impact Model Intercomparison Project (ISIMIP2b), Geosci. Model Dev., 10, 4321–4345, https://doi.org/10.5194/gmd-10-4321-2017, 2017.

Gerten, D., Heck, V., Jägermeyr, J., Bodirsky, B. L., Fetzer, I., Jalava, M., Kummu, M., Lucht, W., Rockström, J., Schaphoff, S., and Schellnhuber, H. J.: Feeding ten billion people is possible within four terrestrial planetary boundaries, Nat. Sustain., 3, 200–208, https://doi.org/10.1038/s41893-019-0465-1, 2020.

Guerra, C. A., Rosa, I. M. D., Valentini, E., Wolf, F., Filipponi, F., Karger, D. N., Xuan, A. N., Mathieu, J., Lavelle, P., and Eisenhauer, N.: Global vulnerability of soil ecosystems to erosion, Landsc. Ecol., 35, 823–842, https://doi.org/10.1007/s10980-020-00984-z, 2020.

Heck, V., Hoff, H., Wirsenius, S., Meyer, C., and Kreft, H.: Land use options for staying within the Planetary Boundaries – Synergies and trade-offs between global and local sustainability goals, Glob. Environ. Change, 49, 73–84, https://doi.org/10.1016/j.gloenvcha.2018.02.004, 2018.

Humphrey, V., Zscheischler, J., Ciais, P., Gudmundsson, L., Sitch, S., and Seneviratne, S. I.: Sensitivity of atmospheric CO2 growth rate to observed changes in terrestrial water storage, Nature, 560, 628–631, https://doi.org/10.1038/s41586-018-0424-4, 2018.

IPCC: Land–climate interactions, in: Climate Change and Land: IPCC Special Report on Climate Change, Desertification, Land Degradation, Sustainable Land Management, Food Security, and Greenhouse Gas Fluxes in Terrestrial Ecosystems, Cambridge University Press, 131–248, https://doi.org/10.1017/9781009157988.004, 2022.

IPCC: Climate Change 2023: Synthesis Report. Contribution of Working Groups I, II and III to the Sixth Assessment Report of the Intergovernmental Panel on Climate Change [Core Writing Team, H. Lee and J. Romero (eds.)]. IPCC, Geneva, Switzerland, IPCC, https://doi.org/10.59327/ipcc/ar6-9789291691647, 2023.

Issaka, S. and Ashraf, M. A.: Impact of soil erosion and degradation on water quality: a review, Geol. Ecol. Landscapes, 1, 1–11, https://doi.org/10.1080/24749508.2017.1301053, 2017.

Ito, A., Nishina, K., Reyer, C. P. O., François, L., Henrot, A.-J., Munhoven, G., Jacquemin, I., Tian, H., Yang, J., Pan, S., Morfopoulos, C., Betts, R., Hickler, T., Steinkamp, J., Ostberg, S., Schaphoff, S., Ciais, P., Chang, J., Rafique, R., Zeng, N., and Zhao, F.: Photosynthetic productivity and its efficiencies in ISIMIP2a biome models: benchmarking for impact assessment studies, Environ. Res. Lett., 12, 085001, https://doi.org/10.1088/1748-9326/aa7a19, 2017.

Iturbide, M., Gutiérrez, J. M., Alves, L. M., Bedia, J., Cerezo-Mota, R., Cimadevilla, E., Cofiño, A. S., Di Luca, A., Faria, S. H., Gorodetskaya, I. V., Hauser, M., Herrera, S., Hennessy, K., Hewitt, H. T., Jones, R. G., Krakovska, S., Manzanas, R., Martínez-Castro, D., Narisma, G. T., Nurhati, I. S., Pinto, I., Seneviratne, S. I., van den Hurk, B., and Vera, C. S.: An update of IPCC climate reference regions for subcontinental analysis of climate model data: definition and aggregated datasets, Earth Syst. Sci. Data, 12, 2959–2970, https://doi.org/10.5194/essd-12-2959-2020, 2020.

Jantz, S. M., Barker, B., Brooks, T. M., Chini, L. P., Huang, Q., Moore, R. M., Noel, J., and Hurtt, G. C.: Future habitat loss and extinctions driven by land-use change in biodiversity hotspots under four scenarios of climate-change mitigation, Conserv. Biol., 29, 1122–1131, https://doi.org/10.1111/cobi.12549, 2015.

Katra, I.: Soil Erosion by Wind and Dust Emission in Semi-Arid Soils Due to Agricultural Activities, Agronomy, 10, 89, https://doi.org/10.3390/agronomy10010089, 2020.

Meehl, G. A., Senior, C. A., Eyring, V., Flato, G., Lamarque, J.-F., Stouffer, R. J., Taylor, K. E., and Schlund, M.: Context for interpreting equilibrium climate sensitivity and transient climate response from the CMIP6 Earth system models, Sci Adv, 6, eaba1981, https://doi.org/10.1126/sciadv.aba1981, 2020.

Montgomery, D. R.: Soil erosion and agricultural sustainability, Proc. Natl. Acad. Sci. U. S. A., 104, 13268–13272, https://doi.org/10.1073/pnas.0611508104, 2007.

Ostberg, S., Lucht, W., Schaphoff, S., and Gerten, D.: Critical impacts of global warming on land ecosystems, Earth Syst. Dyn. Discuss., 4, 541–565, https://doi.org/10.5194/esdd-4-541-2013, 2013.

Pongratz, J., Schwingshackl, C., Bultan, S., Obermeier, W., Havermann, F., and Guo, S.: Land Use Effects on Climate: Current State, Recent Progress, and Emerging Topics, Current Climate Change Reports, 7, 99–120, https://doi.org/10.1007/s40641-021-00178-y, 2021.

Richardson, K., Steffen, W., Lucht, W., Bendtsen, J., Cornell, S. E., Donges, J. F., Drüke, M., Fetzer, I., Bala, G., von Bloh, W., Feulner, G., Fiedler, S., Gerten, D., Gleeson, T., Hofmann, M., Huiskamp, W., Kummu, M., Mohan, C., Nogués-Bravo, D., Petri, S., Porkka, M., Rahmstorf, S., Schaphoff, S., Thonicke, K., Tobian, A., Virkki, V., Wang-Erlandsson, L., Weber, L., and Rockström, J.: Earth beyond six of nine planetary boundaries, Sci Adv, 9, eadh2458, https://doi.org/10.1126/sciadv.adh2458, 2023.

Schaphoff, S., Forkel, M., Müller, C., Knauer, J., von Bloh, W., Gerten, D., Jägermeyr, J., Lucht, W., Rammig, A., Thonicke, K., and Waha, K.: LPJmL4 – a dynamic global vegetation model with managed land – Part 2: Model evaluation, Geosci. Model Dev., 11, 1377–1403, https://doi.org/10.5194/gmd-11-1377-2018, 2018.

Steffen, W., Richardson, K., Rockström, J., Cornell, S. E., Fetzer, I., Bennett, E. M., Biggs, R., Carpenter, S. R., de Vries, W., de Wit, C. A., Folke, C., Gerten, D., Heinke, J., Mace, G. M., Persson, L. M., Ramanathan, V., Reyers, B., and Sorlin, S.: Planetary boundaries: Guiding human development on a changing planet, Science, 347, 1259855–1259855, https://doi.org/10.1126/science.1259855, 2015.

Sterling, S. M., Ducharne, A., and Polcher, J.: The impact of global land-cover change on the terrestrial water cycle, Nat. Clim. Chang., 3, 385–390, https://doi.org/10.1038/nclimate1690, 2013.

Tobian, A., Gerten, D., Fetzer, I., Schaphoff, S., Andersen, L. S., Cornell, S., and Rockström, J.: Climate change critically affects the status of the land-system change planetary boundary, Environ. Res. Lett., 19, 054060, https://doi.org/10.1088/1748-9326/ad40c2, 2024.

Wang-Erlandsson, L., Tobian, A., van der Ent, R. J., Fetzer, I., te Wierik, S., Porkka, M., Staal, A., Jaramillo, F., Dahlmann, H., Singh, C., Greve, P., Gerten, D., Keys, P. W., Gleeson, T., Cornell, S. E., Steffen, W., Bai, X., and Rockström, J.: A planetary boundary for green water, Nat. Rev. Earth Environ., 3, 380–392, https://doi.org/10.1038/s43017-022-00287-8, 2022.

Zhu, J., Penner, J. E., Yu, F., Sillman, S., Andreae, M. O., and Coe, H.: Decrease in radiative forcing by organic aerosol nucleation, climate, and land use change, Nat. Commun., 10, 1–7, https://doi.org/10.1038/s41467-019-08407-7, 2019.